 doi:10.20944/preprints202207.0264.v1

*Article*

# Development and Characterization of Zein/Ag-Sr Doped MBGNs Coatings for Biomedical Applications

**Syeda Ammara Batool [1], Ushna Liaquat [1], Iftikhar Ahmad Channa [2], Sadaf Jamal Gilani [3], Muhammad Atif Makhdoom [4,*], Muhammad Yasir [1], Jaweria Ashfaq [2], May Naseer bin Jummah [3,5,6] and Muhammad Atiq ur Rehman[1,*]**

[1] Department of Materials Science and Engineering, Institute of Space Technology Islamabad, Islamabad 44000, Pakistan; syedaammara001@gmail.com (S.A.B); ushna.ali336@gmail.com (U.L); muhammadyasir85@gmail.com (M.Y)
[2] Thin Film Lab, Department of Metallurgical Engineering, NED University of Engineering and Technology, Off University Road, Karachi 75270, Pakistan; iftikharc@neduet.edu.pk (I.A.C); jaweriaashfaq72@gmail.com (J.I)
[3] Department of Basic Health Sciences, Preparatory Year, Princess Nourah bint Abdulrahman University, Riyadh 11671, Saudi Arabia; sjglani@pnu.edu.sa (S.J.G); mnbinjumah@pnu.edu.sa (M.N.J)
[4] Institute of Metallurgy and Materials Engineering, University of the Punjab Lahore 54590, Pakistan
[5] Biology Department, College of Science, Princess Nourah bint Abdulrahman University, Riyadh 11671, Saudi Arabia.
[6] Environment and Biomaterial Unit, Health Sciences Research Center, Princess Nourah bint Abdulrahman University, Riyadh 11671, Saudi Arabia
* Correspondence: atif.imme@pu.edu.pk (M.A.M); atique1.1@hotmail.com (M.A.R)

**Abstract:** Implants are used to replace damaged biological structures in human body. Although stainless-steel (SS) is a well-known implant material, corrosion of SS implants led to the release toxic metallic ions which produce harmful effects in human body. To prevent material degradation and its harmful repercussions, these implanted materials are subjected to biocompatible coatings. Polymeric coatings play a vital role in enhancing the mechanical and biological integrity of the implanted devices. Zein is a natural protein extracted from corn and is known to have good biocompatibility and biodegradability. In this study, Zein/Ag-Sr doped mesoporous bioactive glass nanoparticles (Ag-Sr MBGNs) were deposited on SS substrates via electrophoretic deposition (EPD) at different parameters. Ag and Sr ions were added to impart antibacterial and osteogenic properties to the coatings, respectively. In order to examine the surface morphology of coatings, optical microscopy and scanning electron microscopy (SEM) were performed. To analyze mechanical strength, pencil scratch test, bend test, corrosion and wear tests were conducted on zein/Ag-Sr doped MBGNs coatings. The results show good adhesion strength, wettability, corrosion, and wear resistance for zein/Ag-Sr doped MBGNs coatings as compared to bare SS substrate. Thus, good mechanical and biological properties were observed for zein/Ag-Sr doped MBGNs coatings. Results suggested these zein/Ag-Sr MBGNs coatings have great potential in bone regeneration applications.

**Keywords:** antibacterial; biomedical implants; electrophoretic deposition; osteogenesis

## 1. Introduction

Biomaterials are the materials that can reside in a biological system to perform a certain function without inducing any toxic effect. They have wide range of applications in bioengineering, pharmaceutics, and biomedical implants, etc. The global biomedical implants market reported to have a worth of ~USD 86 billion in 2019 and anticipated to reach ~USD 147 billion by 2027 with 7.2% growth until 2020-2027. Growth in demographic aging and dire medical conditions influence the recent technological progressions in bioimplants market [1]. The consistent growth in implants market brought the interest of many researchers to this field. Metals, ceramics, polymers, and composites are potentially being used in the fabrication of different types of implants e.g., cardiovascular, orthopedic, cochlear, dental, and etc. Among all the suggested materials, metallic implants are

 doi:10.20944/preprints202207.0264.v1

broadly used in the fabrication of implant devices because apart from being compatible in a biological system, they possess superior mechanical strength as compared to other materials [2]. Foreign body triggers immune system to respond which may result in fibrous encapsulation of foreign body to isolate it from interacting with the biological system [3]. For successful implantation, the implanted material should be familiar to the immune system to respond positively.

Among all metallic implants, stainless-steel (SS) implants have the highest proportion in the fabrication of orthopedic implants due to their cost effectiveness and accessibility. The poor corrosion resistance and relatively higher yield strength of SS implants in physiological environment are the major drawbacks [4, 5]. These implants when interact with a physiological environment either exhibit corrosion or no response. Upon corrosion, SS implants release toxic metal ions (Ni and Cr ions) responsible for infections [6, 7]. Corrosion impairs the function of implants by decreasing cell adhesion and mechanical strength which ultimately leads to implant loosening [8]. The surface coating of SS implants with bio-composites can enhance corrosion resistance and bioactivity of the implants [4, 9].

Biomaterial coatings on metallic implants improve the mechanical as well as biological properties of the implanted devices [10]. These coated materials can either be natural or synthetic depending upon the required properties in the final product. After implantation, the first component that interacts with the implant surface is water followed by the proteins. Thus, it is important to tune the surface of the implant to improve the initial protein attachment [11, 12]. Zein is an alcohol soluble protein which largely contains prolamin. Zein was approved by FDA in 1985 as "generally recognized as safe" excipient. Zein is a natural polymer found in the endosperm cells of corn [13, 14]. Zein contains hydrophobic, neutral amino acids (as leucine, proline, and alanine), and some polar amino acid residues (glutamine). Zein outperforms other proteins because of complete absences of lysine and tryptophan. The solubility of zein is restricted to acetone, acetic acid, aqueous alcohols, and aqueous alkaline solutions owe to the amino acids [15]. Considering the low mechanical strength of biopolymers, they are usually used with bioceramics such as hydroxyapatite (HA) and bioactive glasses (BGs) [16]. BGs are third generation biomaterials having applications in bone tissue engineering. BGs can form strong bond with the natural bone, thus they are considered as bioactive ceramics which are usually used with other polymers [17-19]. Mesoporous bioactive glass nanoparticles (MBGNs) have small pores (2 - 7 nm) in them which increase the surface area of particles, ultimately increasing its reactivity. MBGNs can be loaded with different drugs or metallic ions to facilitate bone tissue engineering, targeted drug delivery, and wound healing [20, 21]. Tabia et al. [22] doped sol-gel derived MBGNs with magnesium and loaded them with Amoxicillin. Results showed controlled drug release and high bioactivity due to the mesoporous structure and composition of BGs. Similarly, Ag and Sr ions doped MBGNs were prepared by [23] using modified Stöber process. Presence of Ag ions impart anti-bacterial properties and Sr ions enhance the osteogenesis by promoting bone regeneration and reducing bone resorption. Various coating techniques are being used to coat bioactive glasses for surface modification such as thermal spraying [24], plasma spraying [25, 26], radio frequency sputtering (RFS) [27, 28], physical vapor deposition (PVD) [29] and electrophoretic deposition (EPD) [30, 31]. EPD is well known for its applications in biomedical coatings [30]. EPD involves the movement and deposition of charged particles from the colloidal suspension in the presence of electric field. EPD is cost effective process conducted at room temperature [32]. Numerous studies are conducted on zein/bioactive glasses composite coatings deposited via EPD [32, 33] but deposition of zein/MBGNs doped with metallic ions via EPD is a new approach to study synergetic effect of dual ions. Evidently, we are the first to present a work on the development of zein/Ag-Sr doped MBGNs coatings deposited on 316L SS via EPD.

In this study, we developed zein/Ag-Sr doped MBGNs coatings on 316L SS substrates via EPD. After developing coatings at designated parameters, coated substrates were

 doi:10.20944/preprints202207.0264.v1

subjected to material characterization. Optical microscopy and scanning electron microscopy (SEM) images verified the uniform deposition on 316L SS substrates.

## 2. Materials and Methods

### *2.1. Materials*

Zein powder (CAS: 9010-66-6), absolute ethanol, acetic acid (all purchased from Sigma-Aldrich®). AISI 316L stainless-steel (addressed 316L SS in this article) foil of ~1mm thickness was used to prepare substrates. The composition of 316L SS was Ni-14.15, Cr-17.75, Mo-2.72, Mn-1.87, Si-0.58, P-0.015, S-0.008, C-0.025, Fe-balance (wt.%). Ag-Sr doped MBGNs were synthesized via modified Stöber process, the details are given in our previous work [23].

### *2.2. Suspension preparation*

Prior to EPD process, a stable suspension of zein/Ag-Sr doped MBGNs was made by following the study conducted by Rivera et.al [33, 34]. Zein powder (6 wt. %) was added in a 100 mL beaker followed by the addition of distilled water (20 wt. %) and absolute ethanol (74 wt. %). The mixture was stirred for 30 min at 35-40 °C on a magnetic hot plate followed by another 30 min round of stirring at room temperature. Acetic acid (~10 mL) was added dropwise to maintain the pH value (~3.0) of the solution. Afterwards, Ag-Sr doped MBGNs (3 g/L) were added in the zein solution followed by 30 min of magnetic stirring. The suspension was finally ultrasonicated for around 60 min to produce a stable suspension of zein/Ag-Sr doped MBGNs required for EPD process. The concentration of Ag-Sr doped MBGNs was chosen on the basis of initial studies, which showed that the concentrations higher than the 3 g/L results in the non-uniform and thick coatings. If the concentration of Ag-Sr doped MBGNs is less than the 3 g/L, it would not be enough to impart bioactivity and antibacterial activity.

### *2.3. EPD process*

316L SS foil was cut into the pieces of 30 x 25 mm2 size. Afterwards, the pieces were cleaned in a mixture of acetone and absolute ethanol. It is important to mention that no surface treatment was carried out on 316L SS foil. Substrates were rinsed with distilled water and dried at room temperature. 316L SS was used as both working and counter electrodes at 10 mm inter-electrode spacing. Both electrodes were then submerged (half of total area) in 50 mL of initially prepared zein/Ag-Sr doped MBGNs suspension. The coatings were developed by applying direct current (DC) on the substrates at different EPD parameters. EPD parameters were chosen on the basis previous literature, which showed that the lower deposition voltages (<10 V) led to the inhomogeneous coatings. In contrast to this, higher deposition voltages (>25 V) led to the pronounced hydrolysis. The range 10-25 V of deposition voltages was investigated in the current study. The deposition time was kept fixed at 180 s on the basis of our previous studies [16].

### *2.4. Materials characterization*

The morphology and chemical composition of synthesized Ag-Sr doped MBGNs were examined via scanning electron microscope (SEM-MIRA, TESCAN) equipped with energy dispersive spectroscopy (EDS).

Samples coated at different parameters were examined under optical microscope (Novex) and SEM to study the morphology and thickness of the coatings. The samples were cut into 5 x 5 mm2 size prior to the examination.

Pencil scratch test (ASTM D3363-20) was conducted to measure the hardness of coatings. This test was performed manually by using graphite pencils of different hardness grade (8B to 2H). Scratches were made by firmly holding pencil at an angle of 45° between the lead tip and the surface of the coated substrates. Starting from most hard (2H) to the softest grade (8B), pencils were pushed to create a scratch by exerting uniform pressure throughout the sample width. The scratches were made until the pencil could not scratch

Preprints (www.preprints.org) | NOT PEER-REVIEWED | Posted: 18 July 2022 doi:10.20944/preprints202207.0264.v1

the surface further. The lowest hardness grade of the pencil that is able to scratch the coating is considered the hardness of the coating. Bend test (ASTM-B571-97) was performed to check the adhesion/bending strength of the coatings. In order to perform the bend test, the coated surface was bent at 180° with the help of tweezers. After bending test, the bending sites were examined to check for defects i.e. cracks and delamination.

Contact angle measurements were done to determine surface wettability. Contact angle measurements were performed by dropping a fixed volume (5 μL) of distilled water via microliter pipette on the surface of coated substrates. Digital images of droplet were captured within 5 s of dropping and the contact angles between the droplet and the surface of the coatings were measured by using Image J™. The test was performed at five different spots on the same coating and the values of contact angles were averaged out. The mean values of contact angles were plotted with their standard deviations.

Tribometer (MT/60/NI, Spain) was used to conduct wear tests on the coated substrates. Ball-on-disk method was used in which a steel ball indenter with a fixed load of 1N was rotated for a distance of 50 m over the surface of the clamped substrates at 32 rpm. A graph between friction coefficient (COF; μ) and partial distance (m) was drawn to understand the wear behavior of the coatings.

Corrosion test was conducted by using three-electrode system Gamry Instrument (potentiostat reference 600, USA). A potentiodynamic polarization scan was recorded in simulated body fluid (SBF). The SBF was prepared by according to the protocol reported in [35]. The composition of SBF is also mentioned in [35]. Coated sample was mounted as working electrode with graphite counter electrode. Ag-AgCl was used as the reference electrode. The test was conducted between the potential range of -0.5 V and +0.5 V at the scan rate of ~1 mV/s. The uncoated side of the substrate was covered with epoxy and dried prior to the test in order to make sure that corrosion results were obtained only from the selected surface area (1 cm2) of the coating. Before conducting this test, open circuit potential (OCP) was measured for an hour. A Tafel plot was constructed by extrapolating the corrosion potential (Ecorr) and corrosion current density (Icorr) curves.

## 3. Results & Discussion

### *3.1. EPD kinetics and suspension stability*

Zein polymer is insoluble in water and organic solvents. It can be dissolved after inducing charge on its functional groups by adding into acidic or basic medium. The polar and nonpolar groups present in zein are protonated in highly pure ethanol (<99%). Next step is to make a stable suspension of zein in ethanol. The stability of the suspension is analyzed using zeta potential measurements. According to the literature, polymer suspension should be sufficiently charged (positively or negatively) for effective electrophoretic mobility [36]. Particles with very low zeta potential tend to agglomerate and settle down due to strong attractive forces of interaction whereas the particles having high values of zeta potential exhibit strong repulsive forces inhibiting the mobility of particles. In case of zein/Ag-Sr doped MBGNs suspension, overall zein and Ag-Sr doped MBGNs are positively charged. Polymeric chain of zein contains some carboxylic side groups that are negatively charged, hence, the zein polymer wraps around the Ag-Sr doped MBGNs due to the attractive forces between oppositely charged side groups [37]. However, resulting zeta potential is positive and zein molecules along with Ag-Sr doped MBGNs move towards cathode and get deposited there following a mechanism termed charge stabilization [38] explained later in kinetics of EPD.

Due to the addition of highly concentrated ethanol (>99%) the zein molecules get protonated and move towards negatively charged electrode, hence resulting in cathodic deposition. Hydrophilic groups of zein make bond with Ag-Sr doped MBGNs and get deposited as single entity. When the electric field is applied, water reduction takes place near cathode and H+ and OH- ions are formed. The pH here increases due to the presence of OH- ions. The positively charged zein/Ag-Sr doped MBGNs get attracted towards the cathode, neutralize with OH- ions, become unstable and get deposited on cathode [39].

Preprints (www.preprints.org) | NOT PEER-REVIEWED | Posted: 18 July 2022 doi:10.20944/preprints202207.0264.v1

*3.2. Morphology of synthesized Ag-Sr doped MBGNs and coatings*

Figure 1 A shows the morphology of the as synthesized Ag-Sr doped MBGNs. The image confirms that the particles were spherical in shape and the average diameter was around 92 nm. The Ag and Sr were detected in the EDS of the particles as shown in Figure 1 B.

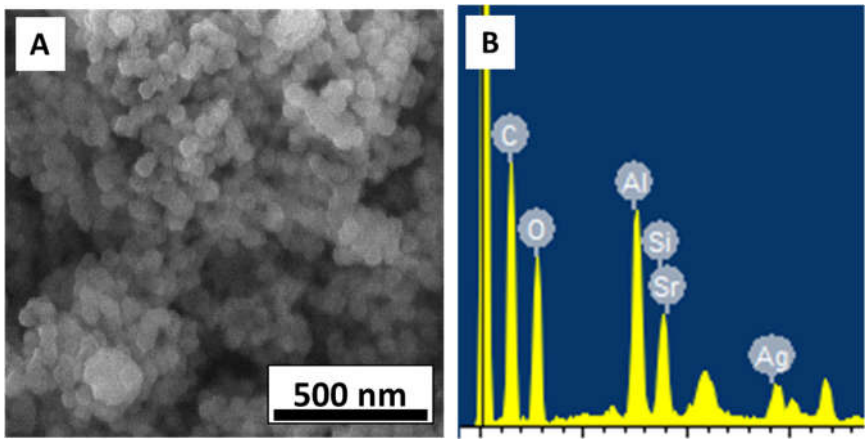


**Figure 1**. (A) SEM image showing spherical morphology of Ag-Sr doped MBGNs, (B) EDS spectrum confirming the doping of Ag and Sr in the bioactive glass network.

Figure 2 show the digital (a-g), optical (h-n), and SEM images (o-u) of zein/Ag-Sr doped MBGNs coatings developed on SS at different voltages. During coating process, a slight change in the color of coatings was observed at 18, 20 and 25 V (Figure 2 e, f, and g). Hydrolysis of suspension seems to be the reason for change in the color of coatings at higher voltages. Hydrolysis causes the chemical breakdown of materials by water. At higher voltages, hydrolysis increases causing rise in the temperature of the suspension. This increase in temperature may lead to the slight change in the color of coatings developed on SS substrates [40].

Further morphological analysis of zein/Ag-Sr doped MBGNs coating was done by using optical microscope and SEM. Figure 2 (h-n) shows the images of zein/Ag-Sr doped MBGNs composite coatings deposited at different parameters taken from optical microscope. Optical micrographs showed uniform dispersion of composite coatings on 316L SS at all the deposition voltages. However, the densest coating was obtained at 25 V/180 s (Figure 2 n) due to high deposition rate at higher value of applied electric field. The similar trend was observed in [16] where the increase in applied electric field led to the increase in deposition yield and density of the coatings. The results of the current study are in agreement with the Hamaker's law [41].

Figure 2 (o-u) shows the SEM micrographs of zein/Ag-Sr doped MBGNs coatings at different voltages. Figure 2 (o and p) shows that Ag-Sr doped MBGNs deposited at 10 V and 12 V were dispersed non-homogenously. A slight increase in voltage up to 14 V and 16 V (Figure 2, q and r) shows large number of zein/Ag-Sr doped MBGNs deposited on SS with enhanced uniformity. At higher voltages of 18, 20 and 25 V, micrographs (Figure 2 s, t, and u) show the highly uniform and homogeneous dispersion of Ag-Sr doped MBGNs within the zein matrix and the coatings were more densely packed. Large spherical agglomerates were formed during electrophoretic deposition process [42]. The thickness of all coatings was measured from the cross section. It was observed that the thickness gradually increased along with the voltage. Figure 2 (v-z2) shows the thickness of coatings deposited at various voltages. The coatings of 9, 11, 12, 14, 15, 22, and 30 μm thickness (average of three values) were obtained at 10, 12, 14, 16, 18, 20, and 25 V, respectively. As the applied voltage increased, more charged particles were forced to move towards the working electrode and deposit there.

Preprints (www.preprints.org) | NOT PEER-REVIEWED | Posted: 18 July 2022 doi:10.20944/preprints202207.0264.v1

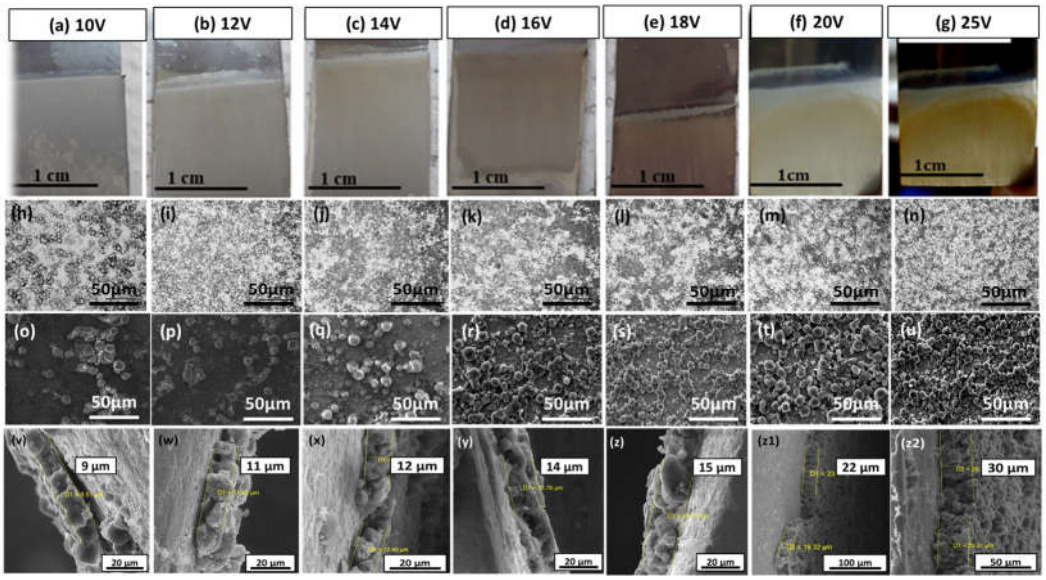


**Figure 2**. Digital images of zein/Ag-Sr doped MBGNs coatings deposited on SS at (a) 10 V, (b) 12 V, (c) 14 V, (d) 16 V, (e) 18 V, (f) 20 V, and (g) 25 V. Optical and SEM images of coatings deposited at 10 V (h, o), 12 V (i, p), 14 V (j, q) and 16 V (k, r) showed non-uniform and less dense coating on SS, respectively. The coatings deposited at 18 V (l, s), 20 V (m, t), and 25 V (n, u) were more uniform and densely packed. The cross sectional images show gradual increase in the thickness of coatings along with the voltage (v-z2).

*3.3 Deposition Yield*

Deposition yield of coatings was calculated by using following formula [43]:

$$\text{Deposition yield} = (\Delta W)/A \ (\text{mg/cm2})$$

Where, $\Delta W$ is the change in the weight of substrates before and after coating and "A" represents the area of coated surfaces. Deposition yield was calculated for each parameter in triplicate and the mean deposition yield (%) was plotted against applied voltages.

Figure 3 shows a consistent increase in the values of deposition yield (%) with the increase in voltage which means that deposition yield is responsive towards the change in voltages. Thus, higher values of deposition yield were obtained at higher voltages (18, 20, and 25 V). The results of this study are in agreement with the Hamaker's law [41].

Preprints (www.preprints.org) | NOT PEER-REVIEWED | Posted: 18 July 2022 doi:10.20944/preprints202207.0264.v1

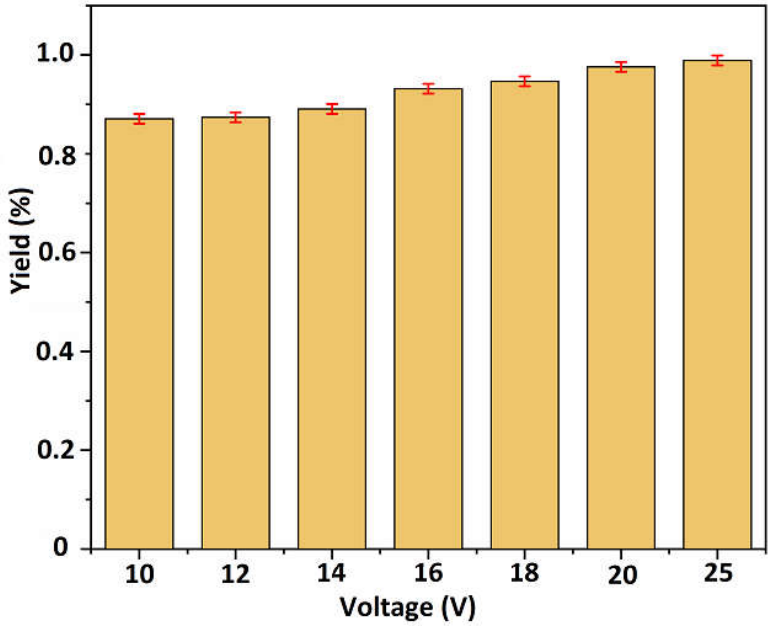


**Figure 3.** Deposition yield (%) graph with respect to the applied voltages. The highest deposition yield was achieved at higher voltage values i.e. 18, 20 and 25 V with slight standard deviations. Deposition yield (%) graph with respect to the applied voltages. The highest deposition yield was achieved at higher voltage values i.e. 18, 20 and 25 V with slight standard deviations.

*3.4. Adhesion Strength*

The adhesion strength of zein/Ag-Sr doped MBGNs coatings deposited on SS was measured by performing pencil scratch test and bend test. Scratches were made on the surface of coated substrates by using graphite pencils of different hardness grade (8B-2H) starting from harder grade, as shown in Figure 4 (a-g). Results of pencil scratch hardness test were then recorded as shown in Table 1. It was observed that coatings developed at higher voltages had higher hardness as compared to those developed at lower voltages. The coating deposited at 25 V was graded 'F' according to the ASTM standard which showed adequate adhesion strength between coating and substrate [44].

Adhesion strength between coatings and substrates was further examined by conducting bend test. The test was performed manually by bending coated substrates at 180° by using tweezers. Figure 4 (h-n) shows the images of the coated substrates taken after conducting bend test. Upon bending, coatings deposited at 10, 12, 14, 16 and 18 V (Figure 4, h-l) showed minor delamination around the edges at bend site. No prominent crack or delamination was observed for coatings deposited at 20 and 25V (Figure 4, m and n) showing good adhesion strength between zein/Ag-Sr doped MBGNs coatings and SS substrates [37, 44]. These coatings were graded '4B' according to the ASTM standard.

Morphological analysis of the coatings revealed that embedded Ag-Sr doped MBGNs in the zein matrix gain in homogeneity with the rise in deposition voltage, as shown in Figure 2 (o-u). Furthermore, the amount of Ag-Sr doped MBGNs within the coatings appear to rise proportionally with the increase in voltage, which could be useful in strengthening the mechanical integrity of the coatings. Due to the increased amount of Ag-Sr doped MBGNs in the coatings, the adhesion strength of the coatings produced at higher voltages was higher than that of the coatings produced at lower voltages [45]. Moreover, the polymeric matrix (i.e. zein) may act as binder, holding the Ag-Sr doped MBGNs on the surface, giving a boost to the mechanical stability of the coatings.

Preprints (www.preprints.org) | NOT PEER-REVIEWED | Posted: 18 July 2022 doi:10.20944/preprints202207.0264.v1

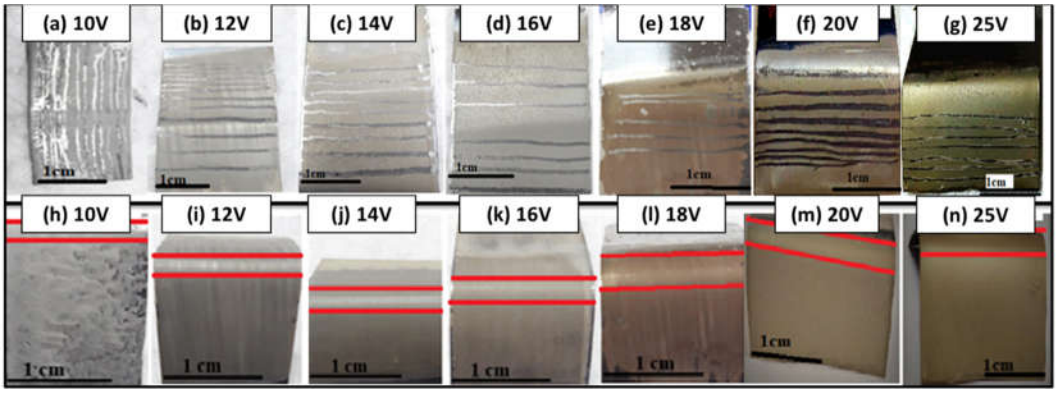


**Figure 4.** Pencil scratch test (a-g) and bend test results (h-n). Coatings deposited at 10 V and 12 V (a and b), detached even with softest pencil i.e. grade 8B, coatings deposited at 14 V (c) detached at 5B, whereas, coatings deposited at 16 V, 18 V (d and e), and 20 V (f) detached at 3B and 1B, respectively. The highest grade was achieved for the coating deposited at 25 V (g). The coatings deposited at 10 V (h), 12 V (i) and 14 V (j) showed delamination and micro-cracks around the bending site. Coatings deposited at 16 V (k) and 18 V (l) showed delamination around the edges of bent site. The coatings deposited at 20 V (m) and 25 V (n) had no delamination or micro-cracks.

**Table 1.** Results of pencil scratch test.

| Voltage (V) | Time (s) | Hardness grade |
|---|---|---|
| 10 | 180 | 8B |
| 12 | 180 | 8B |
| 14 | 180 | 5B |
| 16 | 180 | 3B |
| 18 | 180 | 3B |
| 20 | 180 | 1B |
| 25 | 180 | F |

*3.5. Wettability Studies*

Wettability studies were conducted by performing contact angle measurements on the coated substrates. Surface wettability of implanted materials is vital for successful implantation. When an implanted material enters in physiological environment, it first interacts with body fluids which further allow protein attachment. It is believed that cell adhesion and proliferation depend on the initial protein attachment [46]. If a surface allows initial protein attachment, it will subsequently allow cell adhesion and proliferation. Studies showed the surfaces with a contact angle in range of 35-80° demonstrated good initial protein adsorption and osteoblast cell attachment [47, 48].

Contact angle test was performed on zein/Ag-Sr doped MBGNs coated substrates. The results are plotted between contact angle (◦) and applied voltage (V) along with the standard deviation, as shown in Figure 5. The contact angle was measured five times for each type of coating. Initially, a slight decrease in the values of contact angle was observed up until 16 V and after that, it started increasing. Contact angle at 25 V was measured to be 72 ± 2o which was the greatest among other coatings but perfectly within the suggested range for initial protein and osteoblast cell attachment.

The hydrophilicity of the coatings increases with the rise in applied voltage. This behavior is attributed to the enhanced deposition of Ag-Sr doped MBGNs at higher voltages. The MBGNs are majorly composed of silica network. Silanol (Si-OH) groups present on the surface of silica make it intrinsically hydrophilic [49]. As the amount of MBGNs increases in the coating, its hydrophilic character also increases as compared to the coatings with lower amounts of MBGNs [50].

Preprints (www.preprints.org) | NOT PEER-REVIEWED | Posted: 18 July 2022 doi:10.20944/preprints202207.0264.v1

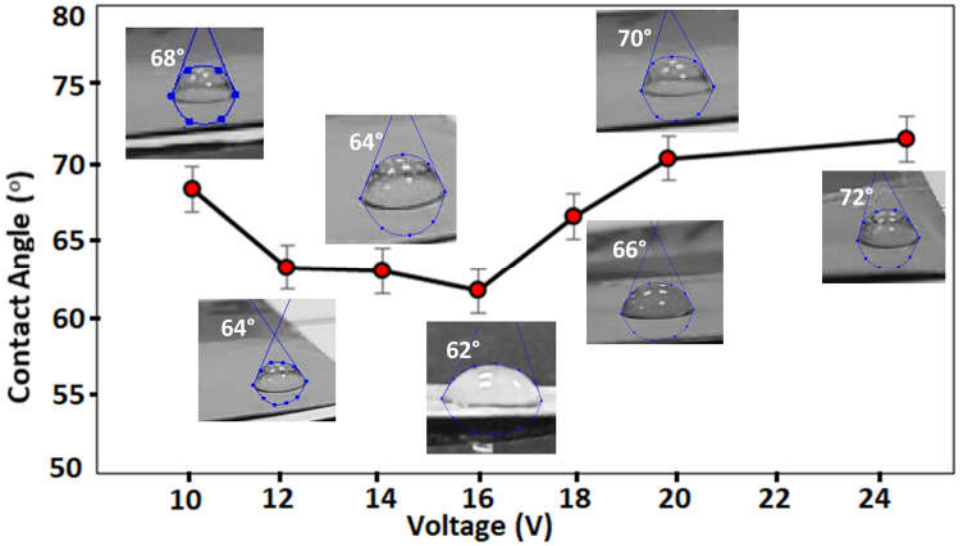


**Figure 5.** Contact angle graph for coatings deposited at different voltages. Highest contact value was obtained for coating deposited at 25 V.

*3.6. Wear Studies*

As discussed earlier, the highest deposition yield and best adhesion results were found for the coating deposited at 25 V for 180 s Thus, wear studies were conducted only for the coatings deposited at 25 V by using ball-on-disk method on a Tribometer. Steel ball indenter was rotated over the surface of coating by applying a load of 1 N for a partial distance of 50 m. A graph was plotted between COF (μ) and partial distance (m), as shown in Figure 6. The graph shows that COF remained almost constant initially, however, there was an abrupt increase in COF around 15 m of partial distance. This behavior may be attributed to the removal of transfer layer between contacting surfaces [51]. A transfer layer is formed due to the accumulation of the wear debris around the wear track leading to the abrasive wear. Later, COF lowered and became constant again throughout the partial distance which means that the coating deposited at higher voltage displayed sufficient resistance to wear [52]. The average wear rate of zein/Ag-Sr doped MBGNs coating was calculated to be 0.179 mm3/Nm which shows adequate wear resistance for a biocompatible implant [53].

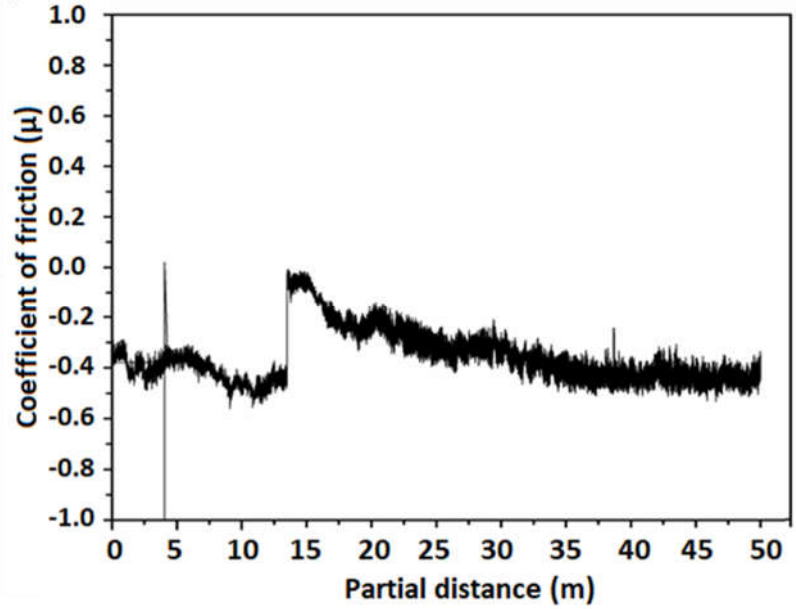


**Figure 6.** Graph between coefficient of friction (μ) and partial distance (m).

Preprints (www.preprints.org) | NOT PEER-REVIEWED | Posted: 18 July 2022 doi:10.20944/preprints202207.0264.v1

*3.7. Corrosion Studies*

To evaluate the corrosion performance of materials, corrosion current ($I_{Corr}$) is measured in a relevant electrolyte. $I_{Corr}$ is the amount of current flowing while corrosion is occurring in an electrochemical cell. Metallic implants with low values of $I_{Corr}$ and high corrosion potential are considered suitable for implantation [54]. Corrosion behavior of zein/Ag-Sr doped MBGNs coatings deposited at 25 V was studied in SBF and compared with the corrosion behavior of bare SS by creating potentiodynamic polarization curve, as shown in Figure 7. A potentiodynamic curve consists of anodic (upper) and cathodic (lower) curves. For better understanding of corrosion behavior, anodic curve is interpreted here. The graph shows the corrosion behavior of both bare SS and coated substrate. The anodic curve of bare SS shows an abrupt increase in the corrosion potential after a certain potential value. This abrupt increase is the indication of breaking of passive layer which prevents corrosion, also reported in our previous study [55]. The breaking of barrier layer results in the accelerated corrosion rate of substrate material. However, the anodic curve of coated substrate shows no blunt increase in the values of corrosion potential.

For further understanding of corrosion behavior of these coatings, the Tafel plot was fitted on these potentiodynamic curves by using Echem™ software. $I_{Corr}$ and corrosion rate (CR) for both bare and coated SS were calculated by the software. The values of $I_{Corr}$ and CR for zein/Ag-Sr doped MBGNs coating deposited at 25 V were quite low as compared to that of bare SS substrates. Similar trend was observed in another study carried out by Ahmed et al. [16]. Zein/hydroxy apatite coating was deposited over 316L SS. The $I_{Corr}$ was significantly lowered due to the presence of zein as compared to the bare substrate. It was concluded that zein coating effectively increases the resistance against corrosion. Thus, in the present study, the corrosion resistance of the coated substrate was inferred to be higher in physiological environment as compared to the bare SS substrates.

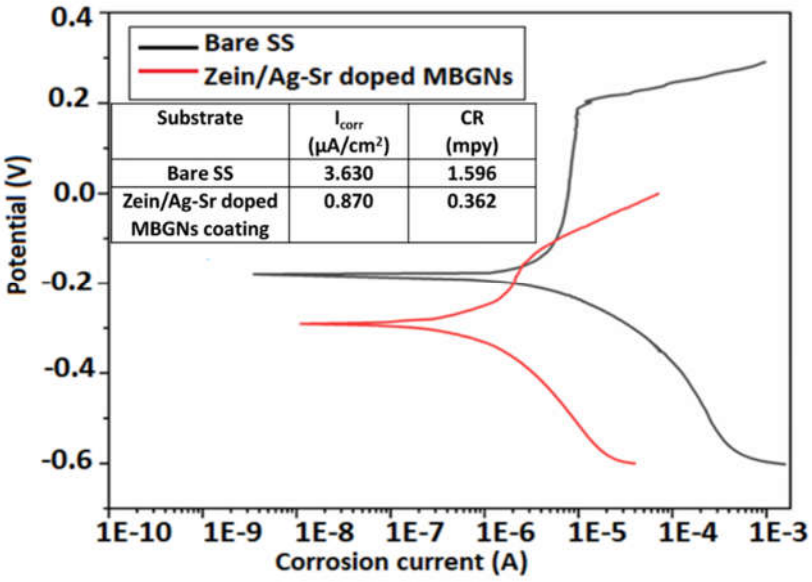


**Figure 7.** Potentiodynamic curves for bare and coated SS substrates.

## 4. Conclusions

In this work, zein/Ag-Sr doped MBGNs coatings were developed on 316L SS by EPD at designated parameters of voltage and deposition time. Following conclusions were obtained at the end of the study.

- High deposition yield of the coatings was obtained at higher voltages i.e. 25 V.
- Optical microscopic images showed uniform deposition of coatings on the surface of SS substrates (at optimum deposition parameter). SEM images illustrated the homogenous distribution of Ag-Sr doped MBGNs throughout the zein matrix along with the

presence of spherical agglomerates indicating good mechanical integration of zein/Ag-Sr dopedd MBGNs coatings.

- Pencil scratch test results showed increased hardness of zein/Ag-Sr doped MBGNs coatings deposited at 25 V from which it was inferred that coatings developed at higher voltage depicted improved adhesion strength. Furthermore, zein/Ag-Sr doped MBGNs coatings exhibited good adhesion strength during bend test.
- Zein/Ag-Sr doped MBGNs coatings deposited at 25 V demonstrated good wettability properties (contact angle of 72 ± 2o) which are suitable for initial protein and subsequent osteoblast cell attachment.
- Moreover, zein/Ag-Sr doped MBGNs coatings showed good wear and corrosion resistance as compared to that of bare SS substrates.

Above mentioned conclusions infer that zein/Ag-Sr doped MBGNs coatings developed in this study via EPD at 25 V exhibited commendable mechanical and surface properties for biomedical applications.

**Author Contributions:** Conceptualization, Syeda Ammara Batool, Ushna Liaquat and Muhammad Atiq ur Rehman; Data curation, Iftikhar Ahmed Channa; Formal analysis, Ushna Liaquat, Iftikhar Ahmed Channa, Muhammad Atif Makhdoom, Muhammad Yasir, Jaweria Ashfaq and May Nasser Bin Jumah; Investigation, Syeda Ammara Batool; Methodology, Syeda Ammara Batool, Sadaf Jamal Gilani, Muhammad Yasir and Muhammad Atiq ur Rehman; Project administration, Muhammad Atiq ur Rehman; Resources, Ushna Liaquat and Jaweria Ashfaq; Writing – original draft, Syeda Ammara Batool and Muhammad Atiq ur Rehman; Writing – review & editing, Sadaf Jamal Gilani, Muhammad Atif Makhdoom and May Nasser Bin Jumah.; All authors have read and agreed to the published version of the manuscript."

**Funding:** Not Applicable

**Institutional Review Board Statement:** Not Applicable

**Informed Consent Statement:** Not Applicable

**Data Availability Statement:** Data available upon request from the corresponding author(s).

**Conflicts of Interest:** The authors declare no conflict of interest.

## References

1. A. S. Sayali Shinde, Onkar Sumant, "Medical Implant Market By Product Type (Orthopedic Implants, Cardiovascular Implants, Spinal Implant, Neurostimulators, Ophthalmic Implants, Dental Implants, Facial Implants, and Breast Implants) and Biomaterial Type (Metallic Biomaterials, Ceramic Biomaterials, Polymers Biomaterials, and Natural Biomaterials): Global Opportunity Analysis and Industry Forecast, 2020–2027," Nov,2020 2020.
2. L. T. Kuhn, "6 - BIOMATERIALS," in Introduction to Biomedical Engineering (Second Edition), J. D. Enderle, S. M. Blanchard, and J. D. Bronzino, Eds., ed Boston: Academic Press, 2005, pp. 255-312.
3. M. Kastellorizios, N. Tipnis, and D. J. Burgess, "Foreign Body Reaction to Subcutaneous Implants," Cham, 2015, pp. 93-108.
4. N. Godbole, S. Yadav, R. Manickam, and S. Belemkar, "A Review on Surface Treatment of Stainless Steel Orthopedic Implants," International Journal of Pharmaceutical Sciences Review and Research, vol. 36, pp. 190-194, 01/03 2016.
5. M. A. Balestriere, K. Schuhladen, K. Herrera Seitz, A. R. Boccaccini, S. M. Cere, and J. Ballarre, "Sol-gel coatings incorporating borosilicate bioactive glass enhance anti corrosive and surface performance of stainless steel implants," Journal of Electroanalytical Chemistry, vol. 876, p. 114735, 2020/11/01/ 2020.
6. I. B. Narmada, R. A. Baya, T. J. J. o. I. D. Hamid, and M. Research, "Nickel and Chromium Ions Release from Stainless Steel Bracket Immersed in Fluoridated Mouthwash," vol. 11, pp. 294-298, 2018.
7. L. Patnaik, S. R. Maity, and S. J. M. T. P. Kumar, "Status of nickel free stainless steel in biomedical field: A review of last 10 years and what else can be done," vol. 26, pp. 638-643, 2020.
8. C. K. Hebert, R. E. Williams, R. S. Levy, and R. L. Barrack, "Cost of Treating an Infected Total Knee Replacement," vol. 331, pp. 140-145, 1996.
9. G. Manivasagam, D. Dhinasekaran, and A. Rajamanickam, "Biomedical Implants: Corrosion and its Prevention -A Review," Recent Patents on Corrosion Science, vol. 2, pp. 40-54, 06/04 2010.
10. A. Nouri and C. Wen, "1 - Introduction to surface coating and modification for metallic biomaterials," in Surface Coating and Modification of Metallic Biomaterials, C. Wen, Ed., ed: Woodhead Publishing, 2015, pp. 3-60.

11. H. P. Felgueiras, J. C. Antunes, M. C. L. Martins, and M. A. Barbosa, "1 - Fundamentals of protein and cell interactions in biomaterials," in Peptides and Proteins as Biomaterials for Tissue Regeneration and Repair, M. A. Barbosa and M. C. L. Martins, Eds., ed: Woodhead Publishing, 2018, pp. 1-27.
12. J. E. Gagner, W. Kim, and E. L. Chaikof, "Designing protein-based biomaterials for medical applications," Acta Biomaterialia, vol. 10, pp. 1542-1557, 2014/04/01/ 2014.
13. R. Paliwal and S. Palakurthi, "Zein in controlled drug delivery and tissue engineering," Journal of Controlled Release, vol. 189, pp. 108-122, 2014/09/10/ 2014.
14. J. Dong, Q. Sun, and J.-Y. J. B. Wang, "Basic study of corn protein, zein, as a biomaterial in tissue engineering, surface morphology and biocompatibility," vol. 25, pp. 4691-4697, 2004.
15. S. Tortorella, M. Maturi, V. Vetri Buratti, G. Vozzolo, E. Locatelli, L. Sambri, et al., "Zein as a versatile biopolymer: different shapes for different biomedical applications," RSC Advances, vol. 11, pp. 39004-39026, 2021.
16. Y. Ahmed and M. A. Ur Rehman, "Improvement in the surface properties of stainless steel via zein/hydroxyapatite composite coatings for biomedical applications," Surfaces and Interfaces, vol. 20, p. 100589, 2020/09/01/ 2020.
17. A. El-Ghannam and P. Ducheyne, "1.9 Bioactive Ceramics," in Comprehensive Biomaterials II, P. Ducheyne, Ed., ed Oxford: Elsevier, 2017, pp. 204-234.
18. T. A. van Vugt, J. A. P. Geurts, J. J. Arts, and N. C. Lindfors, "3 - Biomaterials in treatment of orthopedic infections," in Management of Periprosthetic Joint Infections (PJIs), J. J. C. Arts and J. Geurts, Eds., ed: Woodhead Publishing, 2017, pp. 41-68.
19. S. Zahid, A. T. Shah, A. Jamal, A. A. Chaudhry, A. S. Khan, A. F. Khan, et al., "Biological behavior of bioactive glasses and their composites," RSC Advances, vol. 6, pp. 70197-70214, 2016.
20. W. Huang, J. Yang, Q. Feng, Y. Shu, C. Liu, S. Zeng, et al., "Mesoporous Bioactive Glass Nanoparticles Promote Odontogenesis and Neutralize Pathophysiological Acidic pH," vol. 7, 2020-August-06 2020.
21. Z. Neščáková, K. Zheng, L. Liverani, Q. Nawaz, D. Galusková, H. Kaňková, et al., "Multifunctional zinc ion doped sol - gel derived mesoporous bioactive glass nanoparticles for biomedical applications," Bioact Mater, vol. 4, pp. 312-321, Dec 2019.
22. Z. Tabia, K. El Mabrouk, M. Bricha, and K. Nouneh, "Mesoporous bioactive glass nanoparticles doped with magnesium: drug delivery and acellular in vitro bioactivity," RSC Advances, vol. 9, pp. 12232-12246, 2019.
23. S. Bano, M. Akhtar, M. Yasir, M. Salman Maqbool, A. Niaz, A. Wadood, et al., "Synthesis and Characterization of Silver–Strontium (Ag-Sr)-Doped Mesoporous Bioactive Glass Nanoparticles," vol. 7, p. 34, 2021.
24. R. B. J. S. Heimann and C. Technology, "Thermal spraying of biomaterials," vol. 201, pp. 2012-2019, 2006.
25. R. B. Heimann, Plasma-spray coating: principles and applications: John Wiley & Sons, 2008.
26. R. B. Bourne, C. H. Rorabeck, B. C. Burkart, P. G. J. C. o. Kirk, and r. research, "Ingrowth surfaces. Plasma spray coating to titanium alloy hip replacements," pp. 37-46, 1994.
27. Y. Yang, K. H. Kim, and J. L. Ong, "A review on calcium phosphate coatings produced using a sputtering process--an alternative to plasma spraying," Biomaterials, vol. 26, pp. 327-37, Jan 2005.
28. J. L. Ong, L. C. Lucas, W. R. Lacefield, and E. D. Rigney, "Structure, solubility and bond strength of thin calcium phosphate coatings produced by ion beam sputter deposition," Biomaterials, vol. 13, pp. 249-254, 1992/01/01/ 1992.
29. R. Sergi, D. Bellucci, and V. Cannillo, "A Comprehensive Review of Bioactive Glass Coatings: State of the Art, Challenges and Future Perspectives," vol. 10, p. 757, 2020.
30. L. Besra and M. J. P. i. m. s. Liu, "A review on fundamentals and applications of electrophoretic deposition (EPD)," vol. 52, pp. 1-61, 2007.
31. A. Boccaccini, S. Keim, R. Ma, Y. Li, and I. J. J. o. t. R. S. I. Zhitomirsky, "Electrophoretic deposition of biomaterials," vol. 7, pp. S581-S613, 2010.
32. A. R. Boccaccini, S. Keim, R. Ma, Y. Li, and I. Zhitomirsky, "Electrophoretic deposition of biomaterials," vol. 7, pp. S581-S613, 2010.
33. L. Ramos Rivera, J. Dippel, and A. R. Boccaccini, "Formation of Zein/Bioactive Glass Layers Using Electrophoretic Deposition Technique," ECS Transactions, vol. 82, pp. 73-80, 2018/01/23 2018.
34. M. Demir, L. Ramos-Rivera, R. Silva, S. N. Nazhat, and A. R. Boccaccini, "Zein-based composites in biomedical applications," vol. 105, pp. 1656-1665, 2017.
35. T. Kokubo and H. Takadama, "How useful is SBF in predicting in vivo bone bioactivity?," Biomaterials, vol. 27, pp. 2907-15, May 2006.
36. C. J. Cheng and O. G. Jones, "Stabilizing zein nanoparticle dispersions with ι-carrageenan," Food Hydrocolloids, vol. 69, pp. 28-35, 2017/08/01/ 2017.
37. S. Kaya and A. R. Boccaccini, "Electrophoretic deposition of zein coatings," Journal of Coatings Technology and Research, vol. 14, pp. 683-689, 2017/05/01 2017.
38. F. Pishbin, A. Simchi, M. P. Ryan, and A. R. Boccaccini, "Electrophoretic deposition of chitosan/45S5 Bioglass® composite coatings for orthopaedic applications," Surface and Coatings Technology, vol. 205, pp. 5260-5268, 2011/09/25/ 2011.
39. M. A. Ur Rehman, "Zein/Bioactive Glass Coatings with Controlled Degradation of Magnesium under Physiological Conditions: Designed for Orthopedic Implants," Prosthesis, vol. 2, 2020.

40. J. G. Speight, "Chapter 3 - Industrial Organic Chemistry," in Environmental Organic Chemistry for Engineers, J. G. Speight, Ed., ed: Butterworth-Heinemann, 2017, pp. 87-151.
41. H. C. Hamaker, "Formation of a deposit by electrophoresis," Transactions of the Faraday Society, vol. 35, pp. 279-287, 1940.
42. Q. Nawaz, S. Fastner, M. A. U. Rehman, S. Ferraris, S. Perero, G. G. di Confiengo, et al., "Multifunctional stratified composite coatings by electrophoretic deposition and RF co-sputtering for orthopaedic implants," Journal of Materials Science, vol. 56, pp. 7920-7935, 2021/05/01 2021.
43. M. A. U. Rehman, F. E. Bastan, B. Haider, A. R. J. M. Boccaccini, and Design, "Electrophoretic deposition of PEEK/bioactive glass composite coatings for orthopedic implants: A design of experiments (DoE) study," vol. 130, pp. 223-230, 2017.
44. M. A. U. Rehman, M. A. Munawar, D. W. Schubert, and A. R. Boccaccini, "Electrophoretic deposition of chitosan/gelatin/bioactive glass composite coatings on 316L stainless steel: A design of experiment study," Surface and Coatings Technology, vol. 358, pp. 976-986, 2019/01/25/ 2019.
45. M. Atiq Ur Rehman, F. E. Bastan, B. Haider, and A. R. Boccaccini, "Electrophoretic deposition of PEEK/bioactive glass composite coatings for orthopedic implants: A design of experiments (DoE) study," Materials & Design, vol. 130, pp. 223-230, 2017/09/15/ 2017.
46. R. Aqib, S. Kiani, S. Bano, A. Wadood, and M. A. Ur Rehman, "Ag–Sr doped mesoporous bioactive glass nanoparticles loaded chitosan/gelatin coating for orthopedic implants," International Journal of Applied Ceramic Technology, vol. 18, pp. 544-562, 2021/05/01 2021.
47. J. D. Bumgardner, R. Wiser, S. H. Elder, R. Jouett, Y. Yang, and J. L. Ong, "Contact angle, protein adsorption and osteoblast precursor cell attachment to chitosan coatings bonded to titanium," J Biomater Sci Polym Ed, vol. 14, pp. 1401-9, 2003.
48. J. Wei, T. Igarashi, N. Okumori, T. Igarashi, T. Maetani, B. Liu, et al., "Influence of surface wettability on competitive protein adsorption and initial attachment of osteoblasts," Biomed Mater, vol. 4, p. 045002, Aug 2009.
49. J. Laskowski and J. A. Kitchener, "The hydrophilic—hydrophobic transition on silica," Journal of Colloid and Interface Science, vol. 29, pp. 670-679, 1969/04/01/ 1969.
50. J. Wu, K. Xue, H. Li, J. Sun, and K. Liu, "Improvement of PHBV Scaffolds with Bioglass for Cartilage Tissue Engineering," PLOS ONE, vol. 8, p. e71563, 2013.
51. N. A. Masripan, Y. Miyahira, H. Nishimura, T. Tokoroyama, N. Umehara, and Y. Fuwa, "Effect of Transfer Layer on Ultra Low Friction of CNx Coating under Blowing Dry Ar," Tribology Online, vol. 8, pp. 219-226, 05/15 2013.
52. S. Waqar, A. Wadood, A. Mateen, and M. A. U. Rehman, "Effects of Ni and Cr addition on the wear performance of NiTi alloy," The International Journal of Advanced Manufacturing Technology, vol. 108, pp. 625-634, 2020/05/01 2020.
53. R. S. Virk, M. A. Rehman, M. A. Munawar, D. W. Schubert, W. H. Goldmann, J. Dusza, et al., "Curcumin-Containing Orthopedic Implant Coatings Deposited on Poly-Ether-Ether-Ketone/Bioactive Glass/Hexagonal Boron Nitride Layers by Electrophoretic Deposition," Coatings, vol. 9, 2019.
54. N. Eliaz, "Corrosion of Metallic Biomaterials: A Review," Materials (Basel, Switzerland), vol. 12, p. 407, 2019.
55. M. A. Ur Rehman, F. E. Bastan, A. Nawaz, Q. Nawaz, and A. Wadood, "Electrophoretic deposition of PEEK/bioactive glass composite coatings on stainless steel for orthopedic applications: an optimization for in vitro bioactivity and adhesion strength," The International Journal of Advanced Manufacturing Technology, vol. 108, pp. 1849-1862, 2020.